Proceedings of the 41st IEEE
Conference on Decision and Control
Las Vegas, Nevada USA, December 2002

Convergence design considerations of low order Q-ILC for closed loop systems, implemented on a high precision wafer stage.

B.G.Dijkstra[1], O.H.Bosgra
Mechanical Engineering
Systems and Control Group,
Delft University of Technology
Mekelweg 2, 2628 CD Delft,
The Netherlands
www.ocp.tudelft.nl\sr\BGDijkstra
Email: B.G.Dijkstra@wbmt.tudelft.nl

Abstract

Iterative Learning Control (ILC) design is quite often based on the principle of using the tracking error of a system to obtain an ideal input to reduce the tracking error of the system. For a closed loop system this may not be an optimal choice. In this paper will be shown that in a closed loop setting, using the tracking error signal for ILC may result in conflicting feedback and feedforward actions. This can be avoided by adding frequency weighting to the measured errors but in this paper will be shown that the ILC can be designed without any extra filters by considering what the desired ILC behavior should be and choosing the input signal accordingly. The measured results of two quadratic criterion ILC designs will be presented, only differing in the choice of the input for the ILC, yet still yielding considerably different results.

The designs have been implemented on a high precision wafer stage with direct links to modern wafer steppers used in IC manufacture. The results from these experiments will be used to illustrate the influence of the design choice of the input signal for the ILC.

1 Introduction

Iterative Learning Control (ILC) design is quite often based on the principle of using the tracking error of a system to obtain an ideal input to reduce the tracking error of the system ([1], [2],[3], [4], [5], [6]). In an open loop situation this is quite an obvious design choice, but for a system that contains a feedback controller this choice is not so straightforward. When designing an ILC based on a quadratic criterion (Q-ILC), the convergence behavior of the ILC is determined by the choice of the weightings, which result in a trade-off between the input effort / noise amplification, and the tracking error. These weightings are shaped by the model of the system used during ILC design, and can have a considerable effect on the convergence behavior of the ILC. By choosing a different output for an ILC, these weightings can be modified into a more desirable form without the need for any additional frequency filters. This illustrates that the initial design choice of input output signals for ILC can, and should, be used to shape its behavior.

In previous publications ([6], [7]) has been shown that for LTI models an optimal control design based on a quadratic criterion can be exactly described with a low order LTI model of the system. This makes the use of Q-ILC much more appealing since it eliminates the need for solving a very high dimensional control problem. In this paper this low order Q-ILC design method will be used.

First the low order Q-ILC design method is briefly discussed, followed by an introduction to the experimental wafer stage that has been used for the implementation of the designs. In the following section two different designs will be presented followed by the experimental results for these two designs. The results show that the desired ILC behavior should be taken into account when designing the iterative learning controller since the resulting performance is for a large part determined by the choice of the input of the iterative learning controller.

[1]This research project is being sponsored by Philips CFT

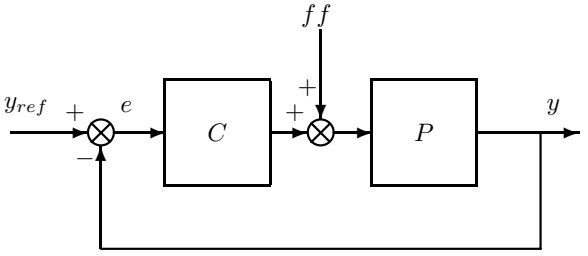

Figure 1: Closed loop system of the wafer stage. P denotes the waferstage, C the feedback controller

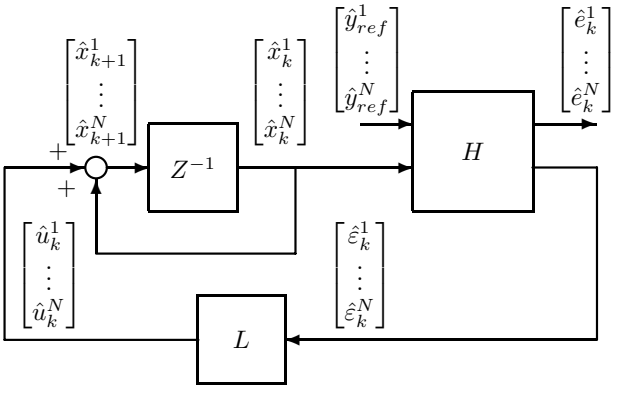

Figure 2: Iterative Learning Control setting.

2 Low order Q-ILC design

The Q-ILC design discussed in this paper is a low order design as described in [6],[7] which is equivalent to a full order Linear Quadratic optimal control design as discussed in e.g. [5], [2],[3].

Consider the closed loop system in figure 1, where C denotes a feedback controller and P denotes the plant under consideration (a wafer stage in this case). ILC will be used to obtain a feedforward signal (ff) that results in minimal tracking error (e) with respect to the desired trajectory (y_{ref}). A general ILC set-up is shown in figure 2, where the the system has two inputs, $\hat{y}_{ref}$ and $\hat{x}_k$ (the feedforward signal ff). All signals denoted in figure 2 are vectors of length N describing a finite discrete time signal. The blocks are system descriptions defined over a finite interval of length N. These blocks can be considered a large impulse response matrices or as any other model defined over a finite interval. Note that for a causal LTI system, such a matrix will be a lower triangular Toeplitz matrix containing the Markov parameters of the LTI system.

The index k denotes the trial index of the ILC, so the block Z^{-1} denotes one trial delay for the entire input vector. The trajectory $\hat{y}_{ref}$ is the desired trajectory that does not change from trial to trial, therefore it is a constant vector. This vector introduces an error in the output ($\hat{e}_k$) of the system which needs to be suppressed, so effectively this constant disturbance (constant vector from trial to trial) needs to be suppressed in the output $\hat{e}_k$ (the tracking error). To this end, according to the internal model principle [8], a model describing this constant is needed: a bank of N discrete time integrators, shown in figure 2 with the feedback around delay Z^{-1}.

The ILC (L) is designed by optimal control methods minimizing the criterion:

$$J = \sum_{k=1}^{M} \hat{\varepsilon}_k^T Q \hat{\varepsilon}_k + \hat{u}_k^T R \hat{u}_k \tag{1}$$

For the rest of the paper define:

$$\begin{aligned} \hat{\varepsilon}_k &= H_1 \hat{x}_k \quad R = \beta \\ Q &= \left(H_1^T H_1 + \beta^2 I \left(H_1^T H_1 + 2\beta I \right)^{-1} \right) \end{aligned} \tag{2}$$

Again, H_1 is a large matrix and and for a SISO system β will be a scalar. The optimal solution with this weighting is defined by the Riccati equation:

$$-S\left(\beta I + S\right)^{-1} S + Q = 0 \tag{3}$$

with feedback interconnection:

$$L = S^{-1} H_1^T \tag{4}$$

and solution to the Riccati equation (3):

$$S = H_1^T H_1 + \beta I \tag{5}$$

In general this Riccati equation will be of very large order since the matrices S,H and Q will have dimensions of $N \times N$, which is very large for anything but short trajectories.

In [6] has been shown that for LTI systems the solution from 5 can be exactly calculated using the simulation of a Hamiltonian system, where only a state space model of system H_1 (A, B, C) and the relative weighting (β) is needed, which is not very numerically demanding:

$$\begin{bmatrix} I & B\beta^{-1}B^T \\ 0 & A^T \end{bmatrix} \begin{bmatrix} x(l+1) \\ p(l+1) \end{bmatrix} = \begin{bmatrix} A & 0 \\ -C^T C & I \end{bmatrix} \begin{bmatrix} x(l) \\ p(l) \end{bmatrix} + \begin{bmatrix} \beta^{-1}B \\ 0 \end{bmatrix} y(l) \tag{6}$$

$$u(l) = \beta^{-1} y(l) - \beta^{-1} B^T p(l+1)$$

These two coupled state equations can be decoupled with the stable poles in Z_{11} and the unstable poles in

Z_{22}:

$$\begin{bmatrix} z(l+1) \\ \tilde{z}(l+1) \end{bmatrix} = \begin{bmatrix} Z_{11} & 0 \\ 0 & Z_{22} \end{bmatrix} \begin{bmatrix} z(l) \\ \tilde{z}(l) \end{bmatrix} + T^{-1} \begin{bmatrix} \beta^{-1}B \\ 0 \end{bmatrix} y(l) \quad (7)$$

$$u(l) = \beta^{-1}y(l) - \beta^{-1}B^T \left(T_{21}z(l) + T_{22}\tilde{z}(l)\right)$$

with the transformation:

$$\begin{bmatrix} z(l) \\ \tilde{z}(l) \end{bmatrix} = T^{-1} \begin{bmatrix} x(l) \\ p(l) \end{bmatrix} \quad (8)$$

$$T = \begin{bmatrix} I & 0 \\ X & I \end{bmatrix} \begin{bmatrix} I & \mathcal{P} \\ 0 & I \end{bmatrix} = \begin{bmatrix} T_{11} & T_{12} \\ T_{21} & T_{22} \end{bmatrix} \quad (9)$$

where X and $\mathcal{P}$ are defined by the discrete Riccati equation:

$$X = A^T XA - A^T XB(\beta - B^T XB)^{-1}B^T XA + Q \quad (10)$$

and the Sylvester equation:

$$Z_{11}\mathcal{P} - \mathcal{P}Z_{22} + Z_{12} = 0 \quad (11)$$

where:

$$\begin{aligned} Z_{11} &= \left(I + B\beta^{-1}B^T X\right)^{-1} A \\ Z_{22} &= {Z_{11}}^{-T} \\ Z_{12} &= -B\beta^{-1}B^T A^{-T} \end{aligned} \quad (12)$$

The stable part of this system Z_{11} can be simulated in positive time direction, and the unstable part Z_{22} in reverse direction. The start conditions of these simulations can be calculated using the transition matrices defined by:

$$\Phi(i, i_0) = Z^{i-i_0} \quad (13)$$

yielding:

$$\Phi_{11}(i, i_0) = Z_{11}^{i-i_0} \quad (14)$$

$$\Phi_b(N, 0) = \sum_{j=0}^{N-1} \Phi_{11}(N, j+1)T^{-1} \begin{bmatrix} \beta^{-1}B \\ 0 \end{bmatrix} y(j) \quad (15)$$

$$z(N) = \Phi_{11}(N, 0)z(0) + \Phi_b(N, 0) \quad (16)$$

$$\Phi_{\tilde{b}}(0, N) = \sum_{j=0}^{N-1} \Phi_{22}(0, j+1)T^{-1} \begin{bmatrix} \beta^{-1}B \\ 0 \end{bmatrix} y(j) \quad (17)$$

$$\tilde{z}(0) = \Phi_{22}(0, N)\tilde{z}(N) + \Phi_{\tilde{b}}(0, N) \quad (18)$$

$$x(0) = \begin{bmatrix} T_{11} & T_{12} \end{bmatrix} \begin{bmatrix} z(0) \\ \tilde{z}(0) \end{bmatrix} \quad (19)$$

$$p(N) = \begin{bmatrix} T_{21} & T_{22} \end{bmatrix} \begin{bmatrix} z(N) \\ \tilde{z}(N) \end{bmatrix} \quad (20)$$

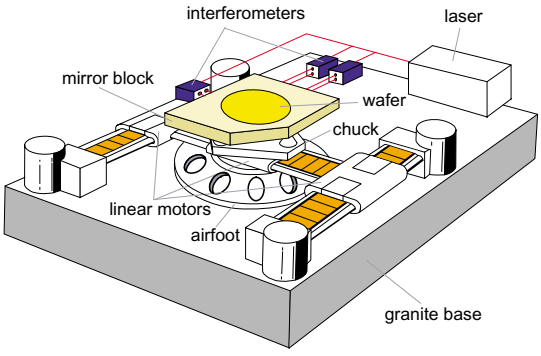

Figure 3: Wafer stage of a wafers stepper
picture is shown by courtesy of D.de Roover [1]

or equivalently:

$$\begin{bmatrix} T_{11} & T_{12} & 0 & 0 \\ 0 & 0 & T_{21} & T_{22} \\ -\Phi_{11}(N, 0) & 0 & 1 & 0 \\ 0 & 1 & 0 & -\Phi_{22}(0, N) \end{bmatrix} \begin{bmatrix} z(0) \\ \tilde{z}(0) \\ z(N) \\ \tilde{z}(N) \end{bmatrix} = \begin{bmatrix} x(0) \\ p(N) \\ \Phi_b(N, 0) \\ \Phi_{\tilde{b}}(0, N) \end{bmatrix} \quad (21)$$

The right side of this equality consists of known variables. Note that $x(0) = 0$ and $p(N) = 0$.

3 Experimental set-up

The ILC methods discussed in this paper have been applied in one direction (single input, single output) of a high precision wafer stage as shown in figure 3. This machine consists of a large granite base with a moving mass on top of it (the chuck) that is actuated by linear electro-motors. The granite base is fitted with compliant dampers to the ground to isolate it from outside disturbances. The measurement system consists of laser-interferometers which measure the position of a reflective surface on the sides of the table. This experimental setup is an industrial grade wafer stage, very similar to modern wafer stages used in IC production, which shows the relevance for industrial application.

The system contains a PID feedback controller for disturbance suppression and for stability. The system has force (current) as input and position measurement as output so the system description contains at least a double integrator, which is quite common for motion systems. The closed loop model of the system is shown in figure 5. During the lithographic process of IC manufacture the chuck, holding a silicon disk, is repeatedly moved from one position to the next position

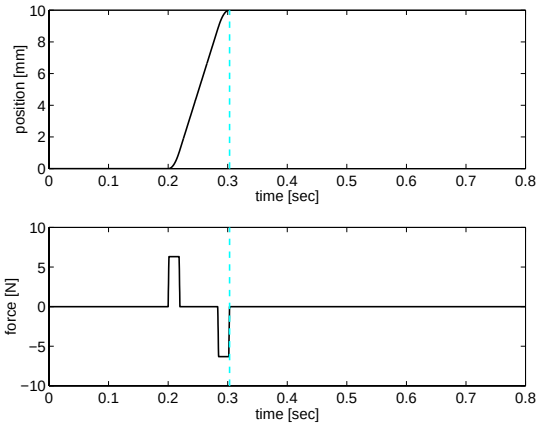

Figure 4: trajectory with initial force feedforward.

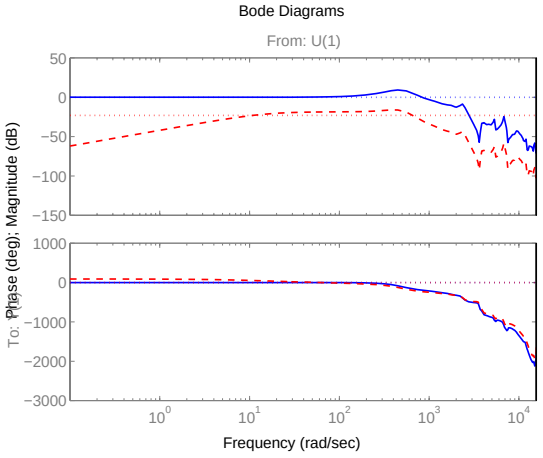

Figure 5: Bode plots of *Design 1* (dashed, $\frac{P}{1+PC}$) and *Design 2* (solid, $\frac{PC}{1+PC}$). Horizontal lines denote the corresponding values of β

to expose each part of the silicon disk in sequence. The trajectory considered is a single one of such steps of the wafer stage, a 3rd order profile based on the physical and practical limitations of the sensors and actuators. The exposure of the IC, can only occur when the errors are within certain limits after movement, so the errors *after* the step, denoted by the vertical dotted line, are of primary importance here. Figure 4 shows the reference trajectory and the force feedforward signal.

4 Description of the Q-ILC experiments

In the rest of the paper two different possible models for the design of aforementioned ILC are discussed. These designs have been applied on a high precision industrial grade wafer stage discussed in the previous section along a 3rd order step profile. The results of these experiments will be presented in the next section.

Design 1 is based on the tracking error, as is quite common for an ILC design:

$$H_1 = \frac{P}{1+PC} \quad \hat{\varepsilon} = \hat{e}_k \tag{22}$$

with $\beta = 0.01$. With such a design the tracking error $\hat{e}_k$ is used as the input to the ILC feedback interconnection L which seems like a straightforward choice. *Design 2* is based on the output of the feedback controller:

$$H_1 = \frac{PC}{1+PC} \quad \hat{\varepsilon} = C\hat{e}_k \tag{23}$$

with $\beta = 1$. Here the feedback controller output, or the feedback effort, is used as input to the ILC.

The bode plots of these two models are given in figure 5. In [7] was shown that β limits the feedback gain in L based on the magnitude of model H. The corresponding values of β are denoted with the dotted lines.

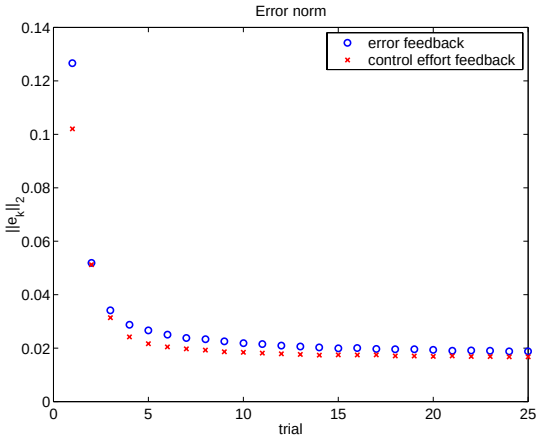

Figure 6: Tracking error norm for *Design 1* (o) and *Design 2* (x).

The different values for β for these 2 designs is due to the difference in overall magnitude of the models. The values have been tuned so that both designs have approximately the same noise suppression and convergence rate as can be shown from the plot of $\|\hat{e}_k\|_2$ from trial to trial in figure 6.

Note that $\hat{\varepsilon}$ in design *Design 2* can be calculated from $\hat{e}_k$ if only this position error is available. The point of this paper however is that $\hat{\varepsilon}$ in design *Design 2* is already directly available without calculations, especially if a digital controller is used.

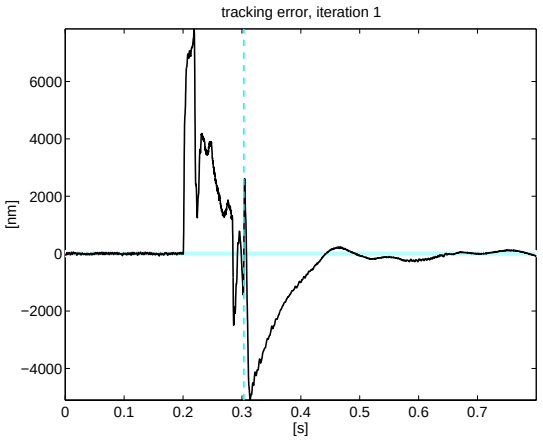

Figure 7: Tracking error for *Design 1*, first trial, in nanometers.

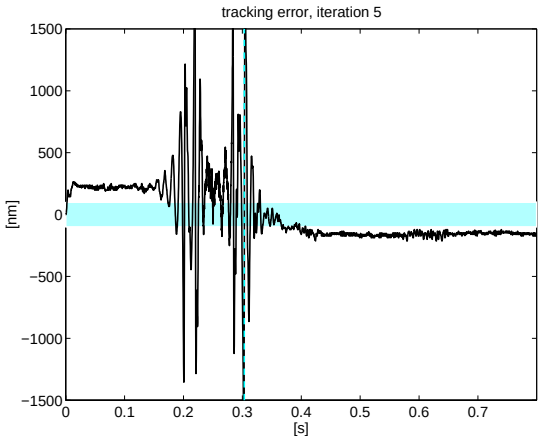

Figure 8: Tracking error for *Design 1*, trial 5, in nanometers.

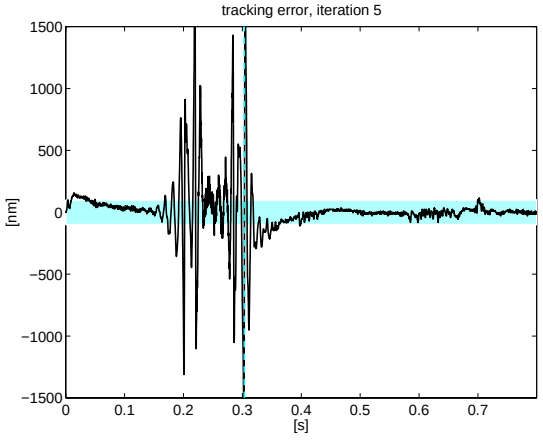

Figure 9: Tracking error for *Design 2*, trial 5, in nanometers.

5 Experimental results

The results presented in this section are measurements from the wafer stage discussed above. First the results of the relatively common *Design 1* are discussed, followed by the results from *Design 2*.

Figure 7 shows the tracking error resulting from the initial feedforward plotted in figure 4. The convergence behavior is mostly interesting in this paper so the results *during* learning, at trial 5, will be plotted to assess the low order Q-ILC behavior. Figure 8 shows a nearly static tracking error, which only slowly disappears as the trials progress. This can be explained by considering the Bode plot of figure 5. The magnitude of the model of *Design 1* shows a roll-off at low frequencies. In the quadratic criterion (1) these low frequencies will not be weighted as much as the mid-range frequencies, resulting in relatively slow convergence for low frequencies (see also [7]). In figure 9 the same measurement is shown for Q-ILC *Design 2*. This figure shows that the low frequency errors are reduced considerably more than with *Design 1*, which again can be explained by looking at the low frequency difference in the Bode plot of figure 5. Even though *Design 2* is not directly aimed at reducing the tracking error $\hat{e}_k$, but at the controller error $C\hat{e}_k$, the tracking error at low frequencies still is reduced faster than with *Design 1*.

The objective for the optimal ILC design (1) will yield a balance between the Iterative Learning Controller effort ($\hat{x}_k$) and the ILC error ($\hat{\varepsilon}_k$). Therefore it is interesting to look at the feedforward signals found by the Q-ILC. Figure 10 shows the output of the feedback controller and the feedforward generated by the Q-ILC of *Design 1*. It can clearly be seen that the feedback and feedforward signals are conflicting in the sense that the output of the feedback controller partly compensates the feedforward signal. With *Design 2*, shown in figure 11 this is no longer the case because the controller effort of the feedback controller is actively weighed in the criterion. Low frequency tracking errors ($\hat{e}_k$) result in large feedback control action due to the presence of the integrating action in the PID controller which is is suppressed more strongly in *Design 2* than in *Design 1*.

After full convergence the resulting tracking error will be nearly identical for both design techniques. If one is specifically interested in reducing low frequency tracking errors fast, it may be a good idea to choose the inputs and outputs used for the ILC not equal to the tracking error itself. The designs shown in this paper are limited to settings where the system dynamics itself are used to shape the Q-ILC behavior, by choosing a different, measurable, output for a different design. This is a very simple choice but not a trivial choice.

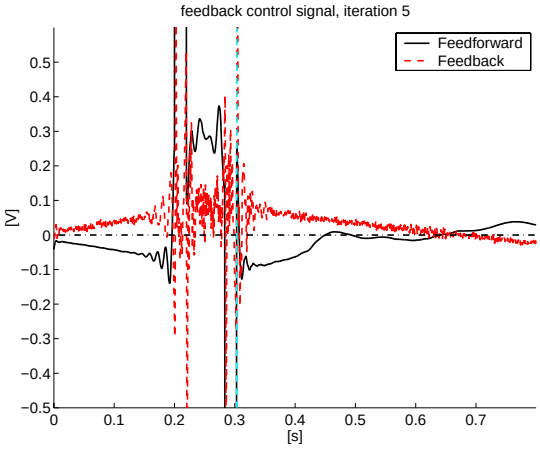

Figure 10: Control signals for *Design 1*, trial 5, in volts.

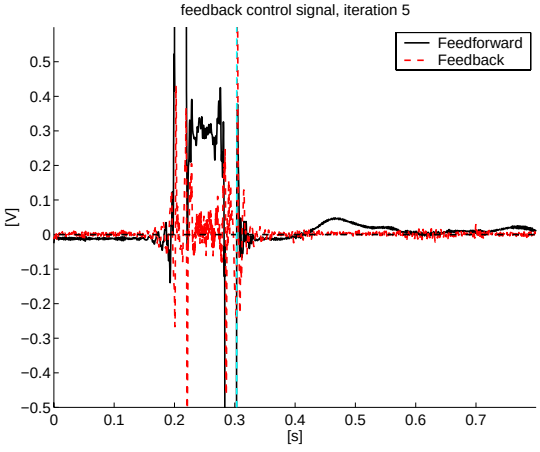

Figure 11: Control signals for *Design 2*, trial 5, in volts.

One should consciously choose the desired convergence *and* converged [7] behavior and choose inputs , weightings and outputs accordingly.

Obviously one can also add frequency dependent weighting (i.e filters) to system measurements to generate an alternative desired output $\hat{\varepsilon}_k$ that may not be available by measurement directly. However, as shown adding such filters may not be at all necessary so before resorting to such techniques it is advisable to consider if the desired properties are not already directly available for measurement.

6 Conclusions

When designing a quadratic criterion based iterative learning controller, one much pay special attention to the design of the weighting in the criterion. In this paper has been shown that by simply choosing a different output measurement the behavior of the ILC can be radically altered.

Some practical insight into the possible design considerations for a Q-ILC, specifically low order Q-ILC for LTI system, has been provided. Choosing the weighting in the quadratic criterion (1) can be nothing more than selecting a specific output with properties corresponding to the desired performance. Before adding extra weighting functions one should consider the possibilities already offered by the closed loop system itself.

The results in this paper illustrate that choosing the inputs for an ILC is not at all self-evident and should be considered carefully.

References

[1] Dick de Roover. *Motion Control of a Wafer Stage. A Design Approach for Speeding Up IC Production.* PhD thesis, Delft University of Technology, 1997. ISBN: [90-407-1562-9].

[2] Jay H. Lee, Kwang S. Lee, and Won C. Kim. Model-based iterative learning control with a quadratic criterion for time-varying linear systems. *Automatica*, 36:641–657, 2000.

[3] Won Cheol Kim, In Sik Chin, Kwang Soon Lee, and Jinhoon Choi. Analysis and reduced-order design of quadratic criterion-based iterative learning control using singular value decomposition. *Computers and Chemical Engineering*, 24:1815–1819, 2000.

[4] Minh Q. Phan, Richard W. Longman, and Kevin L. Moore. Unified formulation of linear iterative learning control. *AAS/AIAA Space Flight Mechanics Meeting, Clearwater, Florida*, Paper No. AAS 00-106, January 2000.

[5] Rob Tousain and Eduard Van der Meché. Design strategies for iterative learning control based on optimal control. *Conference on Decision and Control*, 40:4463–4468, December 2001.

[6] Branko G. Dijkstra and Okko H. Bosgra. Extrapolation of optimal lifted system ILC solution, with application to a waferstage. *American Control Conference*, May 2002.

[7] Branko G. Dijkstra and Okko H. Bosgra. Noise suppression in buffer-state iterative learning control, applied to a high precision wafer stage. *Conference on Control Automation*, September 2002.

[8] B.A. Francis and W.M. Wonham. The internal model principle of control theory. *Automatica*, 12:457–465, 1976.